Journal of
Marine Science and Engineering

MDPI

Article

A Data-Driven DNN Model to Predict the Ultimate Strength of a Ship's Bottom Structure

Im-jun Ban, Chaeog Lim, Gi-yong Kim, Seo-young Choi and Sung-chul Shin *

Department of Naval Architecture and Ocean Engineering, Pusan National University, Busan 46241, Republic of Korea; june3373@pusan.ac.kr (I.-j.B.); orc@pusan.ac.kr (C.L.); yy4893@pusan.ac.kr (G.-y.K.); csyoung@pusan.ac.kr (S.-y.C.)
* Correspondence: scshin@pusan.ac.kr; Tel.: +82-51-510-2525

Abstract: Plates and curved plates are essential components in ship construction. In the design stage, the methods used to evaluate the ultimate strength required to confirm the structural safety of plates include prediction through analytical methods, finite-element analysis (FEA), and empirical formulas. However, with nonlinear buckling, the results of the empirical formula and the FEA differ for small flank angles (1~9). As a result, the prediction of the nonlinear ultimate strength of flank angle (1~9) plates still requires significant computation time and cost. To compensate for this, this study performed an ultimate strength prediction method utilizing a deep neural network together with the 4050 curved plate analysis. In addition, this paper presents the analysis results of the nonlinear finite-element method and the geometric shape and ratio of curved plates as training data. Based on the results of this study, designers can more efficiently design appropriate curved plate members by considering the ultimate strength.

Keywords: buckling; ultimate strength; initial deflection; deep neural network; curved plate; structural analysis

Citation: Ban, I.-j.; Lim, C.; Kim, G.-y.; Choi, S.-y.; Shin, S.-c. A Data-Driven DNN Model to Predict the Ultimate Strength of a Ship's Bottom Structure. *J. Mar. Sci. Eng.* **2024**, *12*, 1328. https://doi.org/10.3390/jmse12081328

Academic Editor: Burak Can Cerik

Received: 5 July 2024
Revised: 1 August 2024
Accepted: 2 August 2024
Published: 6 August 2024

1. Introduction

1.1. Research Background

Plates and curved plates, which are essential components in the construction of ships, are repeatedly subjected to compressive and tensile forces generated by vertical bending moments from lightweight, deadweight, and various degrees of buoyancy. Previous studies have confirmed that nonlinear behavior in curved plates, such as snap-through, snap-back, and secondary buckling, occurs under specific geometric conditions. Consequently, a local strength evaluation should be performed by inspecting the buckling of or collapse of structural elements in the plates and curved plates [1]. In the past century, numerous studies have been performed to determine the ultimate strength behavior, including the critical and elastic buckling strength of plates using various methods [2,3]. To evaluate the safety of plates in the concept of ultimate limit state (ULS) design and analysis, several methods utilize empirical formulas, experimental methods, and the finite-element method (FEM) [4]. Since the early 19th century, various types of empirical formulas have been proposed based on the effective width theory of von Karman, and the verification of this theory has been conducted through experimental and numerical studies by Kármán (1924) [5]. Currently, the FEM, which is considered a powerful technique for performing structural analysis and design, is preferred [6]. Numerical simulation-based structural design has a reasonable cost and calculation time. In addition, high accuracy is preferred when carrying out the infrastructure design of experiments and analyses, and each classification of a ship or shipyard has its own numerical simulation code to suit their needs [7–9]. However, it has a disadvantage in that it requires reinterpretation after changing the geometric dimensions of the plate, owing to the design modification attributed to the change in the ship owner's

requirements and safety concerns. This results in a delay in ship production. In recent years, with the advent of the Fourth Industrial Revolution, there has been ongoing research on the application of artificial intelligence (AI) technology, and the use of big data has been actively applied during the design and construction stages in the shipbuilding industry. The deep neural network (DNN) is an AI technique composed of more than two hidden layers between the input and output layers [10]. In a DNN, after receiving the parameter values from the input layer, the linear combination is processed utilizing nonlinear functions in the hidden layer, is delivered to the output layer, and passes through the activation function. Subsequently, one or various values are printed out. In cases where it was difficult to apply the general analysis procedure because of the complexity of the data, the DNN using regression analysis was effectively utilized. In this study, using the ANSYS nonlinear FEM (NLFEM), we propose a model to predict the ultimate strength of curved plates with varying curvature (1–9), considering the nonlinear behavior of the DNN based on ultimate strength data under uniaxial compression. Using the neural network model proposed in this study, designers can design the plate members of a ship more effectively, in a shorter time and with fewer costs.

1.2. Research Motivation and Methods

Flat and curved plates, which are essential components of a ship, should be able to bear repetitive axial and combined loads and assess structural safety; it is important to estimate their ultimate strength. To do this, there are methods of utilizing the FEM analysis program and proposed empirical formulas, based on experimental results and ALPS/ULSAP [11]. At the design stage, the dimensions and materials of the plate frequently change because of the ship's owner requirements and classification rules. When utilizing a finite-element analysis (FEA) program, changes in the plate dimensions require time for mesh generation and computational cost. The empirical formula can be used solely for specific plate properties or to determine the ultimate strength of a curved plate with a curvature of (1–9). However, plates with nonlinear behaviors estimated by the empirical formula significantly differ from the actual analysis results, leading to low reliability for this method. In this study, the ultimate strength is estimated using a DNN that can find the appropriate regularity using statistical analyses of the parameters and results. In addition, the suitability and need for the learned model are proposed by comparing it with the empirical formulas proposed in previous studies.

Figure 1 illustrates the overall structure of the study. To generate the data utilized for the training of the DNN, the curved plates indicating the nonlinear behaviors, alongside the case utilized for ship construction in the shipyard, were selected before the composition of the neural network model. Structural analysis was performed using ANSYS 2022 R1 software. The verification of the FE model and boundary conditions was confirmed from the results described in previous studies. In this study, the geometry, aspect ratio, and material properties of the curved plate were adopted as parameters. The suitability of the features of the DNN was identified using correlation coefficient analysis. Based on the selected parameters and results, a neural network model was constructed, and the data were classified into data utilized for training and testing. The paper compares the results of the ultimate strength predicted by deep learning with the ANSYS results obtained (structural analysis data) to confirm the prediction accuracy. Finally, the present study compares the existing ultimate strength empirical equations.

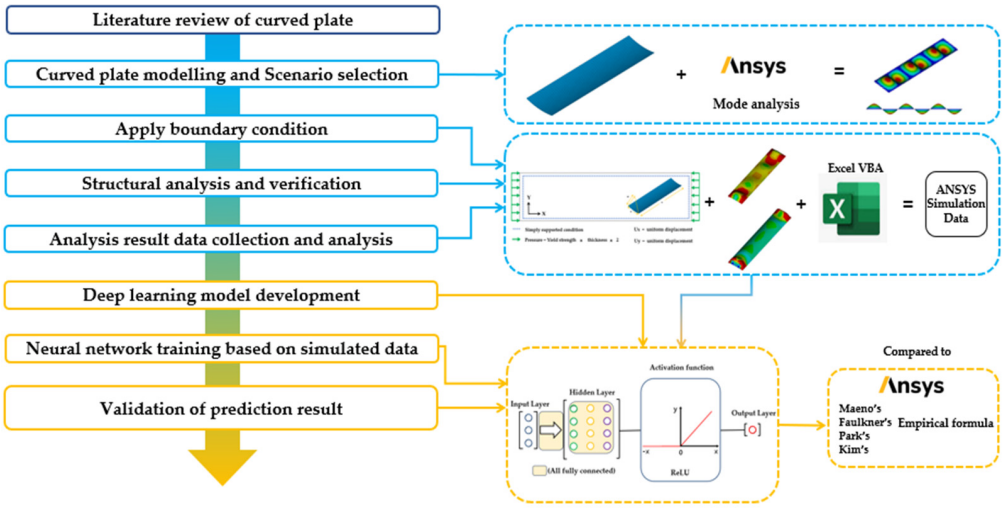

Figure 1. Overall configuration of the research paper.

2. Modeling and Structural Analysis of Curved Plates

2.1. Selection of the Curved Plate Analysis Scenario

To train the neural network, an analysis scenario was selected by referencing the studies of previous researchers. The analysis model, as shown in Figure 2, consists of plate length (a), plate breadth (b), plate thickness (t), and theta (flank angle). A total of 4050 curved plate scenarios were selected with different combinations of geometric shapes, such as length (5), thickness (10), flank angle (9), and initial deflections (3), as proposed by (Smith et al., 1988), and material properties (3), as shown in Equation (1) and Table 1. More detailed scenarios can be found in Appendix A. Initial deflection is a critical factor in the ultimate strength of curved plates, resulting from welding or thermal processing. The formula of initial deflection is shown in Equation (2), which consists of the plate slenderness ratio and plate thickness [12]. Initial deflections are categorized into slight, average, and severe levels. More detailed explanations are provided in Section 2.2. The solution method used for the structural analysis was the arc length method, which is widely used for the buckling analysis of plates. The arc length method used in FEM (finite-element method) is a numerical technique employed to trace the equilibrium path of structures undergoing nonlinear deformations. It is particularly useful for solving problems involving buckling and post-buckling behavior. This method adjusts the load increment and controls the arc length of the solution path, allowing the analysis to progress through limit points and capture the complete load–deformation response of the structure.

$$\left(\begin{matrix} length \\ 5 \end{matrix} \times \begin{matrix} thickness \\ 10 \end{matrix} \times \begin{matrix} flankangle \\ 9 \end{matrix} \times \begin{matrix} initialdeflection \\ 3 \end{matrix} \times \begin{matrix} material \\ 3 \end{matrix} \right) = 4050\ cases \tag{1}$$

$$\omega_{0pl}(initial\ \ deflections) = \begin{cases} 0.025\beta^2 t\ for\ slight\ level \\ 0.1\beta^2 t\ for\ average\ level \\ 0.3\beta^2 t\ for\ severe\ level \end{cases} \tag{2}$$

Generally, as the flank angle of a curved plate increases, the ultimate strength increases. However, in the curvature range of 1–9, nonlinear results are observed (Figure 3). Additionally, nonlinear stress–strain curves, including secondary buckling phenomena such as snap-back and snap-through, complicate the prediction of ultimate strength when using empirical formulas. This phenomenon occurs after buckling due to a compressive load, maintaining in-plane stiffness. It results in a second buckling, which causes a rapid change in in-plane stress distribution due to large deflection. Nonlinear buckling occurs frequently with an aspect ratio of 3, a flank angle of 3–7 and a slenderness ratio of 2.5–4.0. It can also occur under specific conditions outside these ranges [13,14]. This study selected analysis scenarios that include the nonlinear ultimate strength of curved plates.

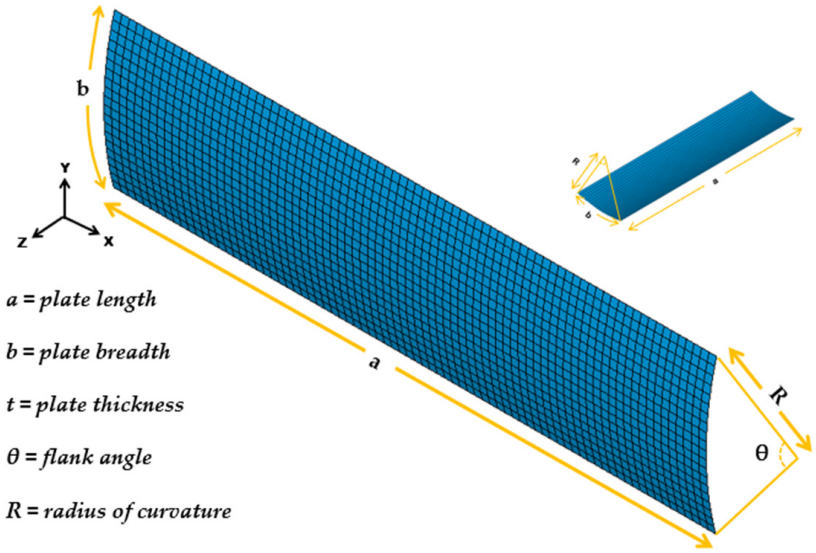

Figure 2. Schematic view of the curved plate.

Table 1. Selected geometric values and materials.

Length (mm); 830, 1660, 2490, 3320, 4150	
Thickness (mm); 235 MPa (7, 10, 13.5, 16.5, 20, 24, 28.5, 32, 36.5, 42)	
	315 MPa (8.5, 12, 15.5, 18.5, 22, 26, 30, 34, 38.5, 44.5)
	335 MPa (9, 12, 17, 19, 23, 26.5, 30.5, 34.5, 42, 50)
Flank angle (°); 1~9	
Material (MPa); 235, 315, 335	

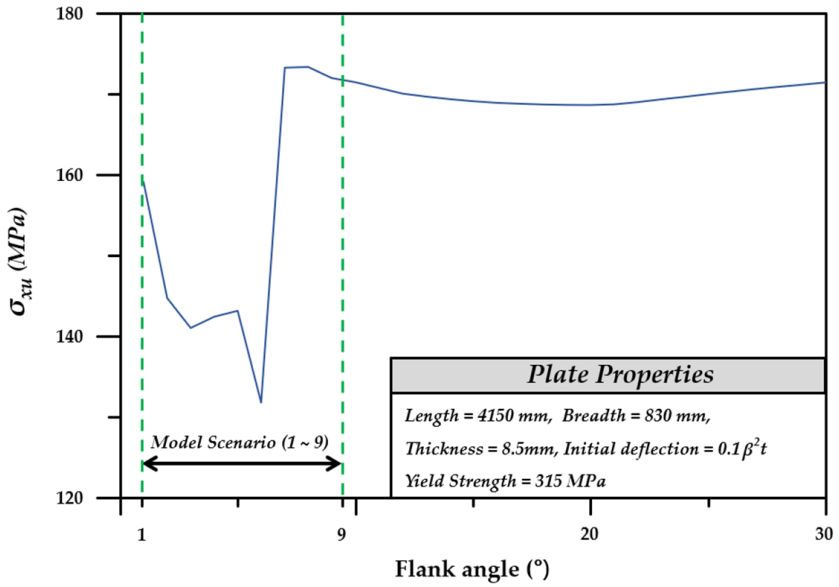

Figure 3. Curved plate scenario selection study.

2.2. Components of the Curved Plate

Yield strength (σ_Y) is a material property that indicates the maximum stress a material can withstand before undergoing plastic deformation. The yield strength of plates used in ship construction is typically 235 MPa, 315 MPa, or 355 MPa. As the yield strength increases, the ultimate strength also increases.

The aspect ratio (α) of the plate is the ratio of its width to its length, and in this study, scenarios 1–5 were utilized. The plate slenderness ratio, as indicated in Equation (3), is

utilized to express the ratio of the thickness to the geometric structure, material properties, and width of the plate. In general, a higher slenderness ratio results in a lower ultimate strength, and the behavior of the ultimate limit state (ULS) is related to the increase in β.

$$\beta = \frac{b}{t}\sqrt{\frac{\sigma_Y}{E}}$$
$$where\begin{Bmatrix} b\ :\ breadth\ of\ plate,\ t\ :\ thickness\ of\ plate \\ \sigma_Y\ :\ yield\ strength,\ E\ :\ young's\ modulus \end{Bmatrix} \quad (3)$$

The curvature of the plate is denoted as r, which is the ratio between the width and radius of the plate, as outlined in Equation (4). In this study, the curvature (1 to 9) that resulted in nonlinear behavior compared to other curvatures was selected. According to the research results of Park, 2018, the secondary buckling phenomenon occurred when the plate curvature was 5, the plate slenderness ratio was 3.45, and the aspect ratio was 3 [15].

$$b = \mathrm{r}\theta$$
$$where\{r = radius\ of\ the\ curved\ plate\} \quad (4)$$

Welding and thermal processing are essential for manufacturing plates and curved plates, and thermal processing causes initial deflections, which affect the ultimate strength of the plate member, and which should be considered for a more accurate analysis. In the case of a flat plate, the initial deflection can be calculated using Equation (2); however, in the curved plate, a shape different from the initial deflection shape of the flat plate is generated owing to the effect of the curvature. Hence, mode analysis was performed and applied to utilize ANSYS. Based on the analysis results, the primary mode shape has the minimum deformation energy and is the most easily deformed. Therefore, applying the primary mode shape, three types of maximum deflections proposed by Smith, 1988, were employed [12]. Table 2 presents the initial deflections of curved plates with different curvatures.

Table 2. Initial deflection of the curved plate.

Initial Deflection Shapes of the Curved Plate					
θ = Flank angle, Scale factor = 200					
θ = 1	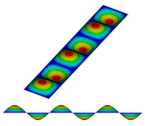	θ = 4	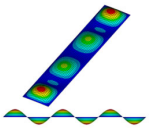	θ = 7	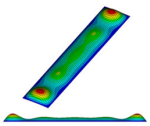
θ = 2	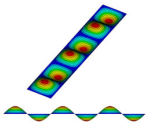	θ = 5	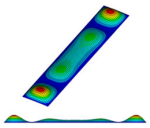	θ = 8	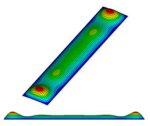
θ = 3	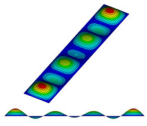	θ = 6	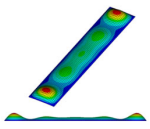	θ = 9	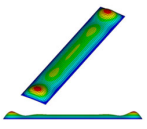

2.3. FE Modeling

During the FEM analysis, the mesh size had a significant impact on the analysis results. Furthermore, the initial deflection occurred in the plate structure, and owing to the welding and thermal processing mentioned above, a relevant initial deflection shape should be considered to obtain accurate analysis results.

Along with the effect of the initial deflection of the mesh, the denser mesh results in FEM values similar to the actual experimental values. Based on the mesh convergence results, a fine mesh leads to lower stress. Figure 4 illustrates the ultimate strength results with different numbers of elements in the width direction of the curved plate, and the

number of elements (NoE) represents the number of elements in the width direction. When the NoE was 6, the highest ultimate strength was observed, and increasing the mesh number decreased the ultimate strength; finally, the ultimate strength converged. With an inadequate amount of mesh, the ultimate strength of the plate is overestimated, leading to inaccurate analysis results [16]. On the contrary, if the number of meshes is too high, each node point generated by the mesh rapidly increases, and the analysis time significantly increases. In this study, the curved plate model was generated by selecting the width-directional mesh as 20, based on the mesh convergence study results, and the aspect ratio of all meshes was set to 1.0 consistently for all analyses.

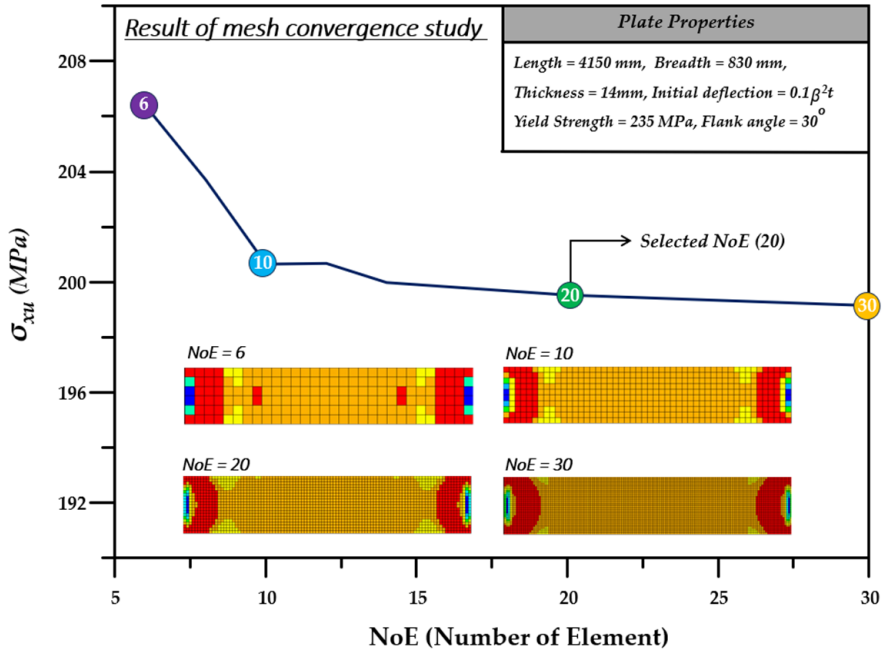

Figure 4. Mesh convergence study result.

2.4. Boundary Conditions of the Curved Plate

The plate utilized in the ship does not have a torsion rigidity of 0 or ∞; it is not a simply supported boundary or clamped boundary condition [17]. However, for the analysis, to investigate the overall behaviors of the plate, including buckling and post-buckling, the two aforementioned boundary conditions are most commonly utilized. Among them, simply supported plates are considered the worst-case scenario and indicate more conservative results compared to the clamped conditions, serving as a criterion for the safety factor [18]. Consequently, simply supported boundary conditions are applied to the four sides, and it is assumed that the plate maintains its straight-line shape (Figure 5). The ship is under various loads because of the bilge cargo and freight. In particular, the plate in the bilge in its hogging state applies a compressive load to the bottom of the ship, owing to the vertical bending moment [19]. The main aim of this study is to determine the ultimate strength of curved plates, considering buckling under a uniform compressive force in the longitudinal orientation.

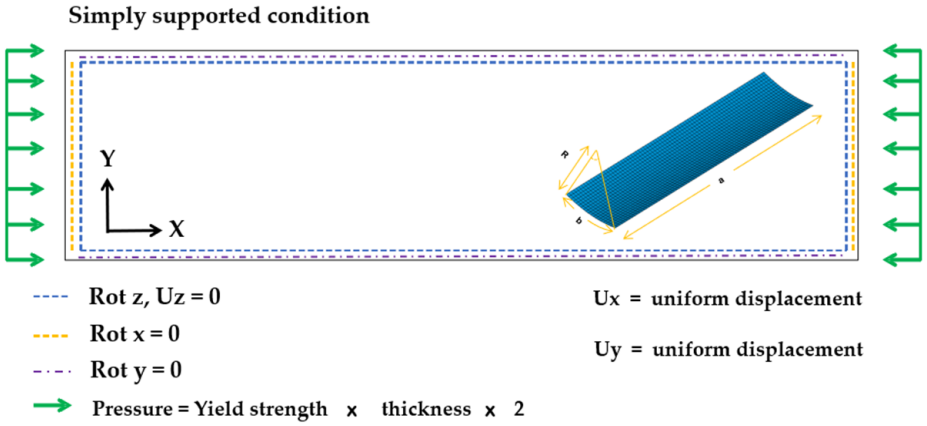

Figure 5. Applied boundary condition of the curved plate.

2.5. Verification of FE Analysis Technique

Before the overall plate scenario analysis, the analysis was performed based on the scenario presented in the study by Park [15]. Then, the results were compared to verify the boundary conditions provided during the modeling and analysis of the plate. The curved plate model in the simply supported longitudinal compression load, which is similar to the boundary conditions of this study, was subjected to a nonlinear structural analysis using ANSYS, and the detailed properties of the plate and materials are presented in Table 3.

Table 3. Selected scenario for the validation of the FE model.

	Geometric Properties					Material Properties		Design Parameter
	a (mm)	**b (mm)**	**t (mm)**	**W_{0pl} (mm)**	**θ (°)**	**σ_Y (MPa)**	**E (GPa)**	**β**
Park (2018) [15]	5000	1000	15	0.15	5	352	205.8	2.7603

Figure 6 illustrates the stress–strain curve of the model used for verification, comparing it with the results [15]. The results showed good agreement. In particular, the secondary buckling, indicating nonlinear behavior under the geometric conditions of the corresponding plate, was identified using the current FE technique. There was a total of 4150 analysis results according to the scenario, and based on the ultimate strength results obtained using different slenderness ratios of the plate, increasing the slenderness ratio of the plate reduced the plate thickness because of the thin cut, in turn decreasing the ultimate strength [20]. As illustrated in Figure 7, when the plate slenderness ratio is below 0.5, it approaches the yield strength of the plate, and with a slenderness ratio greater than 1.0, the ultimate strength rapidly decreases.

The results obtained illustrate the ultimate strength with different initial deflection equations. According to the plate analysis scenarios, three levels—slight, average, and severe—were applied. As illustrated in Figure 8, when the initial deflection value at a slight level was applied, it resulted in the highest ultimate strength compared to a similar plate slenderness ratio [21]. The ultimate strength tended to decrease as the deflection level moved from slight to average and severe. The plate with the severe-level initial deflection had the highest deflection, and its ultimate strength rapidly decreased when the plate slenderness ratio exceeded 1.

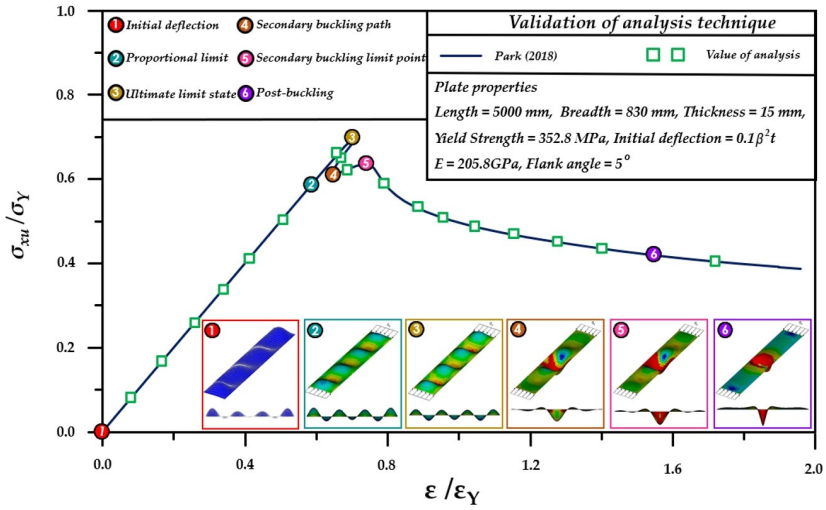

Figure 6. Validation of the ultimate strength of the curved plate [15].

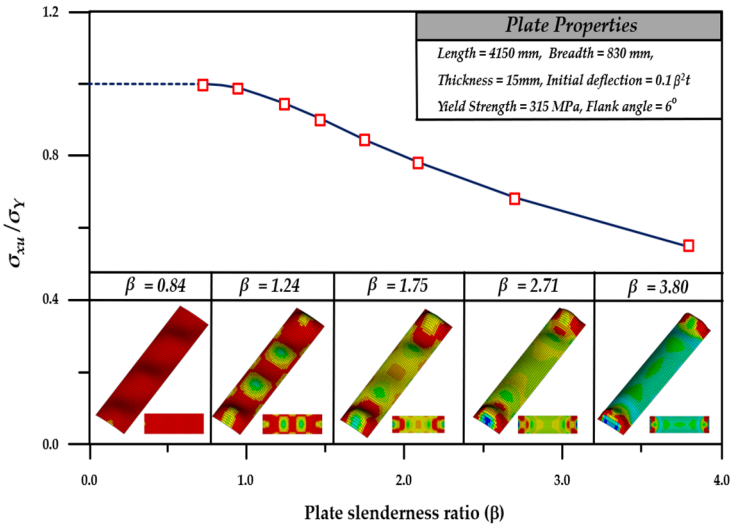

Figure 7. Effect of slenderness ratio on analysis results.

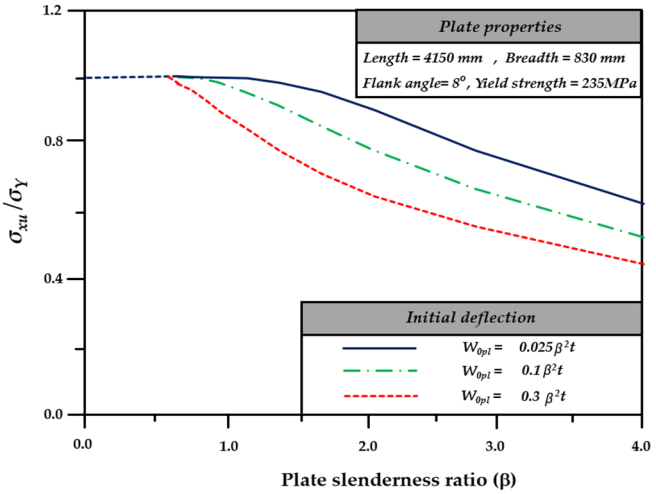

Figure 8. Effect of initial deflection on analysis results.

By compiling the results of 4150 cases, the variables adopted as parameters for deep learning were listed, and based on the analysis results, a total of 67 secondary buckling phenomena were identified. Secondary buckling has an in-plane stiffness against the continuous compressive force even after the buckling occurs, because of the compressive force; then, before it reaches the ultimate strength, another buckling occurs, and the in-plane stiffness rapidly decreases; it then reaches the ultimate strength. Based on its shape, it can be classified as snap-through and snap-back [15]. Figure 9 illustrates the analysis results for the curved plate, presenting snap-through secondary buckling.

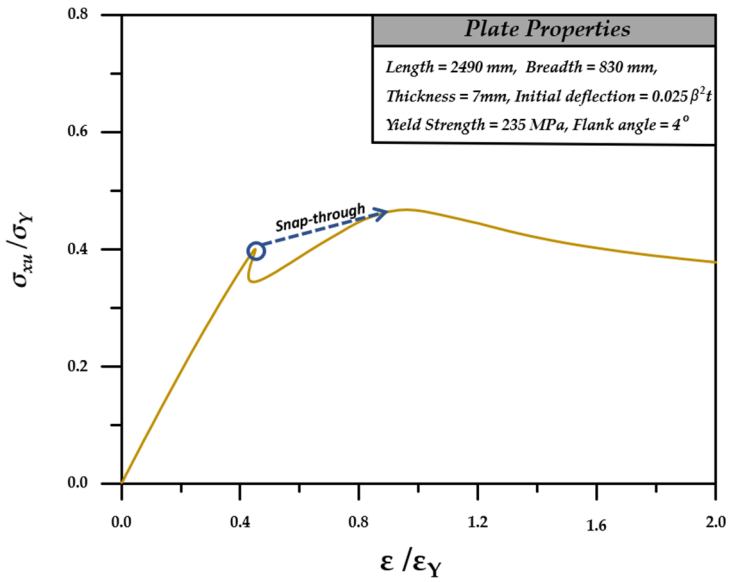

Figure 9. Result of the curved plate with secondary buckling.

3. Development of Deep Learning Model

3.1. Composition of Deep Learning Model

The DNN model was used to predict the ultimate strength of the curved plate, and ten parameters were selected by performing correlation analysis, and the Tensorflow-based Python program was utilized. The overall composition of the neural network comprised the input layer, hidden layers, activation function, and output layer, as illustrated in Figure 10. The input layer receives the values from each parameter and delivers them to the hidden layer; in the hidden layers, the weighted value obtained from the error of the previous learning was modified using the learning rate of the optimization function [22]. The values were then passed through the weighted value of the forward hidden layer, the activation function, and finally delivered to the output layer.

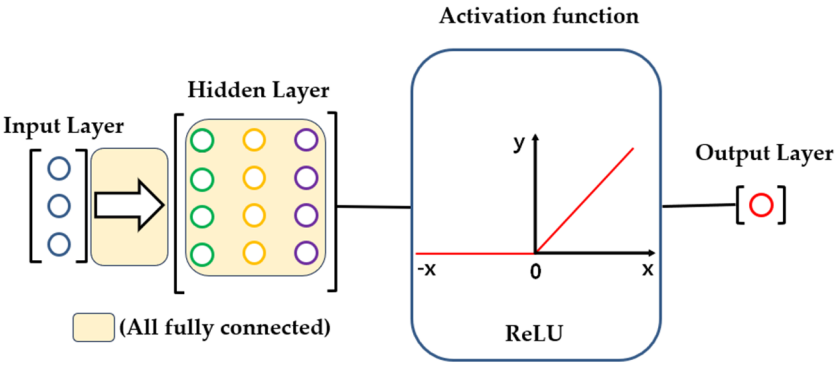

Figure 10. Composition of the DNN model.

As presented in Table 4, the deep learning model was composed of 10 input layers and seven hidden layers, and the weighted value was obtained from the activation function, that is, ReLU, and the ultimate strength value was printed out at the end. The number of hidden layers and nodes utilized were selected, considering the accuracy. For a total of 4050 data points, 80% (3240) were utilized as training data, and 1500 epochs were selected as well. Epoch refers to the number of studies conducted on the total training datasets, and when 3240 datasets are trained once, they are regarded as one epoch. A total of 810 sets of data, excluding those used for learning, were utilized as test data, and the final results were confirmed.

Table 4. Deep learning model structure.

Number of hidden layers	5
Activation function	ReLU
Input features	10
Epoch	1500
No. of training sets	3240
No. of test sets	810

3.2. Selection of Parameters of the Deep Learning Model

The parameters adopted in the deep learning model are the values of the input layer and the factors that significantly impact the output values. The parameters were applied based on the results of the correlation analysis. Correlation is a method of analyzing the linear or nonlinear relationship between two factors, and it can be identified based on the scatter plot and correlation value. Equation (5) shows the correlation coefficient formula, and there are various methods for selecting the features for deep learning training. Among these methods, the correlation coefficient is easy to apply and is widely used [23,24]. A correlation coefficient of 0 indicates no correlation, 0.0–0.2 represents a weak correlation, 0.3–0.5 represents an intermediate correlation, and 0.6–0.9 represents a strong correlation. The correlation coefficient formula is a measure of the strength and direction of the linear relationship between two variables, defined as the covariance of the variables divided by the product of their standard deviations. It provides a quantitative assessment that is particularly useful in feature selection for models, helping to identify which variables have the most significant impact on the target outcome. Table 5 presents the correlation coefficient results of the features with respect to the predicted ultimate strength. Based on these results, the features that demonstrated the highest accuracy in various combinations were selected as follows:

$$correlation\ coefficient = \frac{n(\sum xy)-(\sum x)(\sum y)}{\sqrt{\left[n\sum x^2-(\sum x)^2\right]\left[n\sum y^2-(\sum y)^2\right]}}$$
$$where\left\{\begin{array}{c} n\ :\ number\ of\ data,\ \sum xy\ :\ sum\ of\ the\ product\ data \\ \sum x\ :\ sum\ of\ x\ values,\ \sum y\ :\ sum\ of\ y\ values \\ \sum x^2\ :\ sum\ of\ squares\ x\ values,\ \sum y^2\ :\ sum\ of\ squares\ y\ values \end{array}\right\} \quad (5)$$

Table 5. Correlation analysis for feature selection.

Initial deflection	0.510
Plate length (a)	0.032
Flank angle	0.049
Plate slenderness ratio (β)	0.700
Plate thickness (t)	0.720

Table 5. *Cont.*

Yield strength	0.600
Radius	0.049
Plate length/Radius	0.035
Plate breadth/Radius	0.027
Radius/plate thickness	0.490

3.3. Normalization of Parameter Data

Various ranges of parameters were selected for training an artificial neural network. The parameters related to geometric shape have very high values, while the ratios for the plates have very low values. The scaling effect of these parameters makes learning ineffective. To address this challenge, the data values must be distributed within a fixed range by normalization. Min–max normalization (Equation (6)) and z-score normalization (Equation (7)) were used as the normalization methods [25]. When min–max normalization is applied, the outliers significantly affect the results. Using z-score normalization, outliers are well processed, but similar normalization data cannot be generated. Therefore, normalization should be performed using a suitable method depending on the parameters. In this study, z-score normalization was utilized, and Figure 11 illustrates the normalization results of the parameters.

$$x' = \frac{x - x_{min}}{x_{max} - x_{min}}, \tag{6}$$

$$z = \frac{x - \mu}{\sigma}, \tag{7}$$

where σ is the standard deviation and μ is the mean.

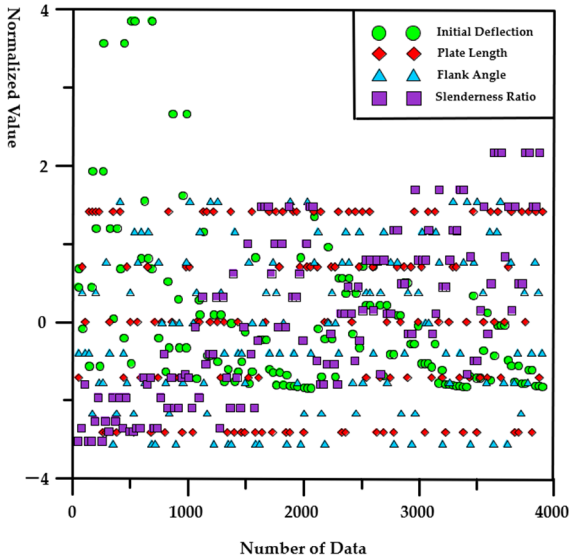

Figure 11. Normalization results of features.

3.4. Loss Function and Optimization Function of the Deep Learning Model

The loss function utilized in the deep learning model in this study is the mean square error, which can evaluate learning by digitizing the difference between the actual and model-predicted values. Sigmoid, tanh, and ReLU are widely used as activation functions. Figure 12 shows the mean square error values of the learning and validation data according to the activation function method. The weighted values obtained from seven input layers and seven hidden layers were processed using the activation function ReLU, and the ultimate strength was printed out. For a total of 4050 sets of data, 80% (3240) were utilized

as learning data, and the learning was performed for 1500 epochs. This model uses the ReLU function (Figure 13), which can solve the vanishing gradient problem of the sigmoid function and has a good convergence speed [26]. The test data evaluated the final performance of the model. An epoch represents the total number of training sets passing through the neural network; one epoch indicates that the total training set was applied to the neural network once, passing through it using forward and backward propagation. Of all the data, 810 datasets, excluding the learning data, were utilized as test data, and the results were verified.

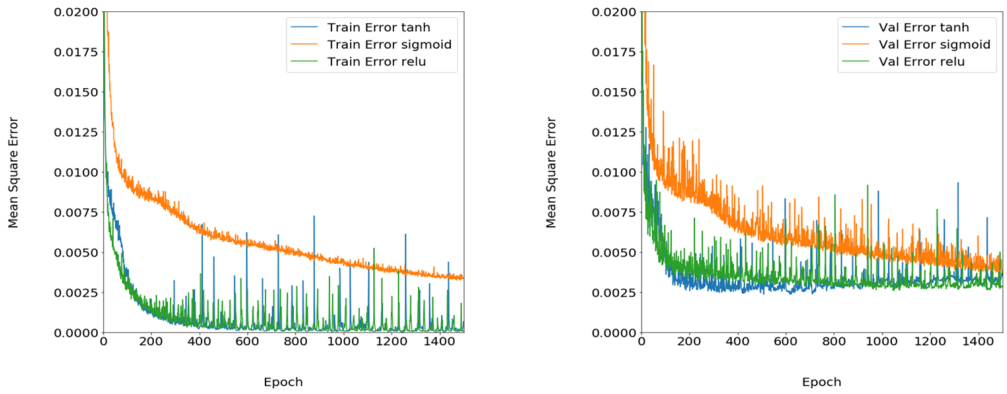

(**a**) MSE of training result (**b**) MSE of validation result

Figure 12. MSE result according to the activation functions.

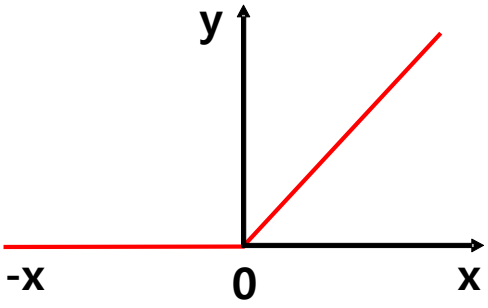

Figure 13. Schematic function of ReLU.

4. Prediction Results of Ultimate Strength Using Deep Learning Model

4.1. Prediction of Ultimate Strength of the Curved Plate

The prediction results of the model that was investigated using deep neural network learning were identified using 810 sets of test data. There were three types of learning results: the prediction results of the total test data, the results for cases in which secondary buckling occurred, and the results of the additional data with different widths that were not studied. Table 6 presents the mean square error (MSE) for every 100 epochs, and it is indicated that the value rapidly converged after 100 epochs. Similarly, Figure 14 illustrates the results of the learning error rate with a function of the epoch value, that is, the number of times studied for the total data. The error value rapidly converged after 100 epochs.

Figure 15 illustrates the comparison results of the values (R^2, MAPE) predicted by the deep learning model (ULS Model) with the analysis results obtained using the NLFEM method (ULS FEM). If there are more values close to the linear graph, the predicted values are in line with the analysis results. Most prediction results indicate high accuracy.

Table 6. Training result for deep learning model.

Epoch	Training Data MSE	Test Data MSE
1	0.4618	0.9370
100	0.0031	0.0049
200	0.0010	0.0044
300	0.0011	0.0047
500	0.0005	0.0028
1300	0.0001	0.0024
1500	0.0001	0.0024

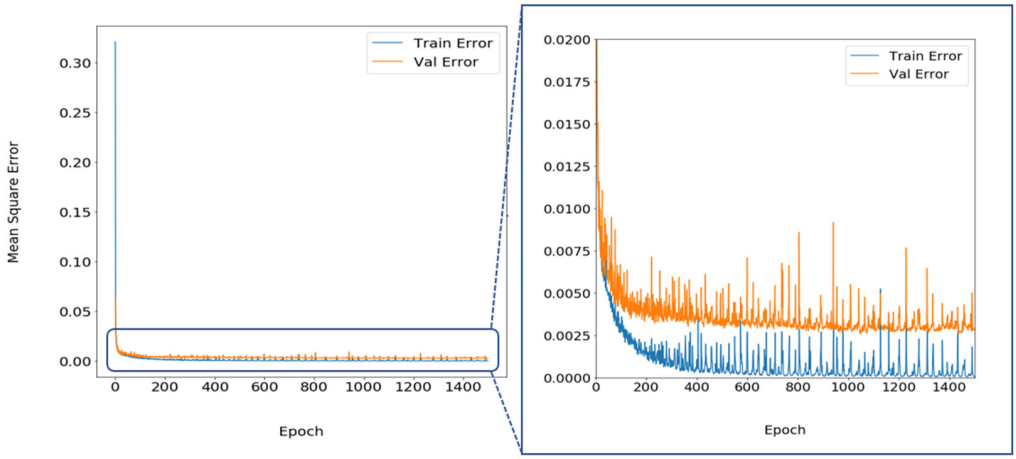

Figure 14. Deep learning model training result.

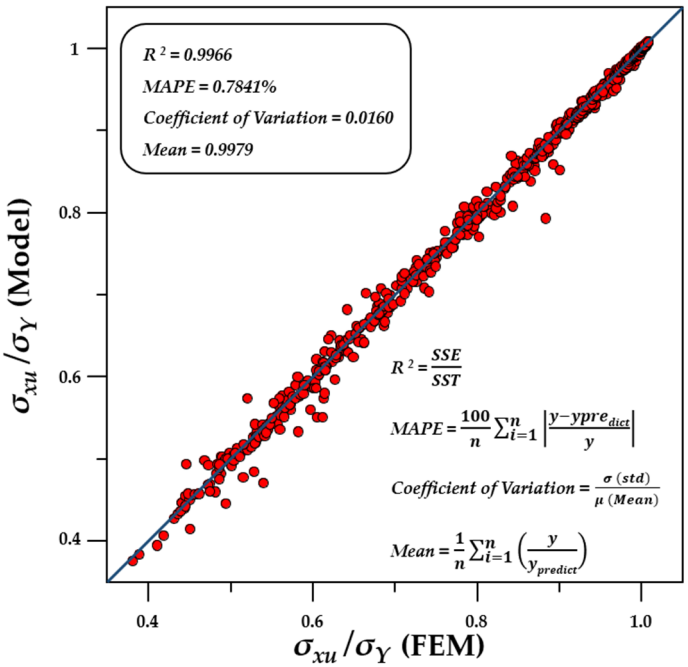

Figure 15. Ultimate strength prediction result of deep learning model (all test data).

Table 7 presents the error of the values predicting the ultimate strength, using the empirical formula obtained from previous studies on the ultimate strength. Because the applicable geometric range of the plate varies for each empirical formula [Equations (8)–(11)],

only the applicable cases were applied and compared by referring to the papers that proposed the empirical formulas [15,21,27,28]. The value predicted using deep learning indicated an average error of 0.86%, which is the most accurate prediction. The average error of the empirical formulas ranges from 2% to 5%, and when there are no limitations or a wide range of applications, the maximum error tends to increase. As mentioned earlier, in the case of a flank angle of 1 to 9, it is determined that the ultimate strength does not increase proportionally with the curvature, but shows significant fluctuations.

Table 7. Comparison of the deep learning model result and empirical formulas (all test data).

Empirical Formula	Average (%)	Max (%)	Min (%)
DNN	0.86	11.63	0.00
Maeno (2004) Equation (8) [27]	2.06	5.11	0.13
Faulkner (1975) Equation (9) [21]	3.67	29.44	0.00
Park (2018) Equation (10) [15]	5.43	20.90	0.00
Kim (2024) Equation (11) [28]	2.16	24.09	0.00

Maeno (2004) [27]

$$\begin{gathered}\frac{\sigma_{xu}}{\sigma_Y} = a\left(\frac{R}{t} - 40\right)^2 + 0.983 \\ \text{where, a} = -0.6\left(\frac{\sigma_Y}{E}\right)^2 + 0.0046\left(\frac{\sigma_Y}{E}\right) - 0.24\left(10^{-6}\right)\end{gathered} \tag{8}$$

Faulkner (1975) [21]

$$\frac{\sigma_u}{\sigma_Y} = \frac{2}{\beta} - \frac{1}{\beta^2} \tag{9}$$

Park (2018) [15]

$$\beta' = \beta \times \sqrt{\frac{\sigma_{CR}^{Flat}}{\sigma_{CR}^{Curve}}}, \qquad \frac{\sigma_u}{\sigma_Y} = \left\{ \begin{array}{ll} 1.0 & for\ \beta < 1.0 \\ \frac{2.0}{\beta'} - \frac{1.0}{\beta'^2} & for\ \beta > 1.0 \end{array} \right\} \tag{10}$$

Kim (2024) [28]

$$\begin{gathered}\frac{\sigma_{xu}}{\sigma_Y} = 1 - \exp\left(\frac{f_1}{\beta} + \frac{f_2}{\beta^2} + \frac{f_3}{\beta^3} + f_4\right) \\ f_1\ to\ f_4 = f(\theta) = A_1\theta^3 + A_2\theta^2 + A_3\theta + A_4 \\ f_1, \quad A_1 = 0, \quad A_2 = -0.02978, \quad A_3 = -0.24789, \quad A_4 = +2.98313 \\ f_2, \quad A_1 = 0, \quad A_2 = +0.02177, \quad A_3 = +0.28736, \quad A_4 = -6.64353 \\ f_3, \quad A_1 = 0, \quad A_2 = 0, \quad A_3 = 0, \quad A_4 = -2.8068 \times 10^{-7} \\ f_4, \quad A_1 = 0, \quad A_2 = +0.00106, \quad A_3 = +0.09659, \quad A_4 = -1.14350 \\ \text{for } flank\ angle,\ 0 \le \theta \le 10\end{gathered} \tag{11}$$

4.2. Prediction of the Ultimate Strength of the Curved Plate in Which Secondary Buckling Occurred

Among the 4050 case analysis results, secondary buckling phenomena were observed in 67 cases. Figure 16 illustrates the stress–strain curves of two plates with identical geometric properties except for curvature, where general and secondary buckling occurred. According to the literature, it is known that secondary buckling occurs in curved plates with an aspect ratio of 3 and a slenderness ratio ranging from 2 to 3.5; however, it also occurs in plates with an aspect ratio of 3–4 and a curvature of 4–7. Although the difference in curvature between the two plates is only 1 and is negligible, their ultimate strengths show a large difference of more than 30 MPa due to secondary buckling. Accordingly, when the ultimate strength was predicted using the empirical formula, it indicated a difference compared to the other curved plates.

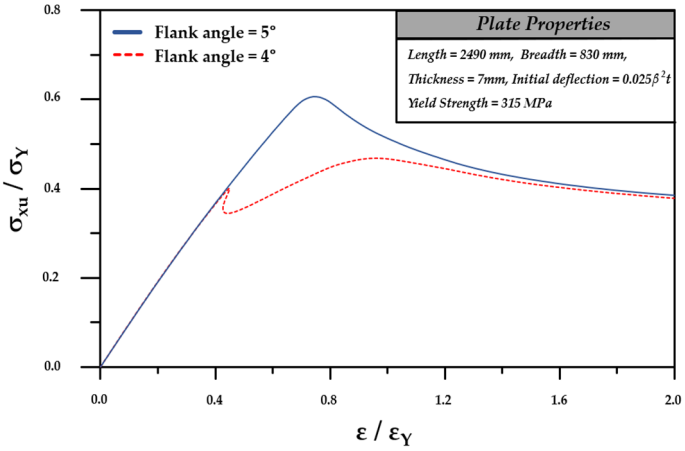

Figure 16. Effect of ultimate strength on secondary buckling.

Although the ultimate strength of most plates linearly increases with increasing curvature, secondary buckling takes place in some cases, and the curvature increases while the ultimate strength decreases. Therefore, for the cases where secondary buckling occurred, the results were investigated using the deep learning model. Figure 17 illustrates the prediction results of the deep learning for the cases where the secondary buckling occurred, and it was confirmed that the deep learning model predicts the ultimate strength of the curved plate where the secondary buckling took place with high accuracy based on the parameters.

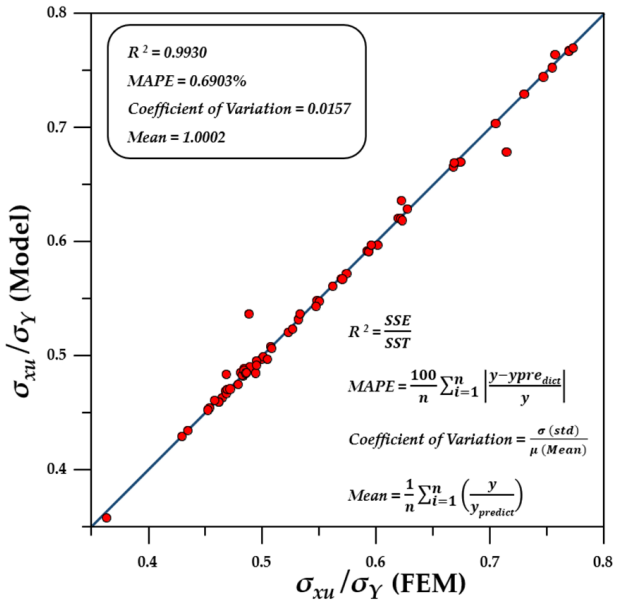

Figure 17. Ultimate strength prediction result of deep learning model (secondary buckling test data).

Table 8 presents the error rates of the ultimate strengths of the plate where secondary buckling occurred, and these were predicted by deep learning and empirical formulas; the empirical formula proposed by Maeno was excluded because there was no applicable plate case. The prediction results showed that the ultimate strength predicted using deep learning had an average error rate of 0.77%, demonstrating the highest accuracy compared to the empirical formulas.

Table 8. Comparison of deep learning model result and empirical formulas (second buckling data).

Empirical Formula	Average (%)	Max (%)	Min (%)
DNN	0.77	9.51	0.00
Maeno (2004) Equation (8) [27]	-	-	-
Faulkner (1975) Equation (9) [21]	8.50	20.25	0.42
Park (2018) Equation (10) [15]	7.41	15.51	0.00
Kim (2024) Equation (11) [28]	7.24	14.03	0.45

4.3. Prediction of Ultimate Strength of Unlearned Curved Plate

The empirical formulas proposed in previous studies have limited ranges for the geometric properties of plates, making it difficult for users to determine a suitable empirical formula. The two aforementioned results obtained utilizing the deep learning model are for the test data and the case where the secondary buckling took place; the plate width was limited to 830 mm. The prediction results of the unlearned width of 1000 mm were investigated to determine the applicable range of the deep learning model for the prediction of the ultimate strength. Figure 18 and Table 9 present the prediction results for a width of 1000 mm obtained without additional learning. Compared with the ultimate strength prediction results obtained for the 830 mm curved plates, the error rates increased. This may be because the correlation between the ultimate strength and the width direction was determined to be 0, indicating an independent relationship; in turn, it was not provided as the input value, and the length of the curved plate was not learned. The average error rate is 2.47%, indicating that it is acceptable for the initial design of the curved plate structure, and can be utilized under non-strict conditions to determine the ultimate strength.

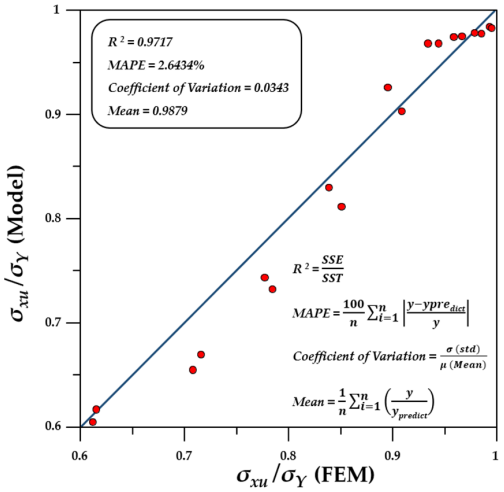

Figure 18. Ultimate strength prediction result of deep learning model (unlearned data).

Table 9. Deep learning model prediction result (unlearned data).

Error	Average (%)	Max (%)	Min (%)
DNN	2.47	7.71	0.05

5. Conclusions

5.1. Overall Summary

In this study, a deep learning model for predicting the ultimate strength was developed by utilizing the nonlinear finite-element analysis results from ANSYS in the scenario of a curved plate under longitudinal compression. By adopting 10 parameters, the ultimate strength was predicted for 810 of the 4050 cases, and the developed model indicated high accuracy compared with the proposed empirical formulas for the cases where the secondary

buckling occurred, and for the plates with different widths that were not included in the learning data. The results of this study can be summarized as follows:

- Utilizing the FEM analysis and empirical formulas, the ultimate strength of the curved plate can be predicted more rapidly compared with nonlinear cases and complicated empirical formulas.
- If the empirical formula is utilized, it can be applied in a limited range of the plate width, length, and slenderness ratio, but it can also predict the ultimate strength of the unlearned plate.
- Based on the prediction results for the ultimate strength of the curved plate utilizing the deep learning model, the developed model indicated a higher accuracy compared with the empirical formulas.

5.2. Limitation of This Study and Future Work

This study has a limitation in terms of obtaining high accuracy and reliability for all the boundary conditions and shapes of various plates. In addition, in some cases, not only for the ultimate strength, but also for the stress–strain curve, strain energy density should be considered when selecting plate members. For future studies, it is suggested that designers can ensure a higher reliability when using this model by providing various analysis results along with the ultimate strength of the plate.

Author Contributions: I.-j.B.: conceptualization, data curation, investigation, methodology, software; C.L.: data curation, validation; G.-y.K.: software, data curation, validation; S.-y.C.: data curation, investigation; S.-c.S.: conceptualization, investigation, project administration, supervision. All authors have read and agreed to the published version of the manuscript.

Funding: This work was supported by the Korea Institute of Energy Technology Evaluation and Planning (KETEP), the Ministry of Trade, Industry, and Energy (MOTIE) of the Republic of Korea (no. 20224000000090) and Korea Institute of Marine Science & Technology Promotion (KIMST) funded by the Ministry of Oceans and Fisheries, Korea (20220210).

Institutional Review Board Statement: Not applicable.

Informed Consent Statement: Not applicable.

Data Availability Statement: The data that support the findings of this study are available from the corresponding author upon the request.

Conflicts of Interest: The authors declare no conflicts of interest.

Appendix A

Table A1. Curved plate scenario with simply supported (a/b = 1, 2, 3, 4, 5).

Yield (MPa)	Length (mm)	Breadth (mm)	Thickness (mm)	Plate Slenderness Ratio
235	830	830	7	4.0067
			10	2.8047
			13.5	2.0776
	1660		16.5	1.6998
	2490		20	1.4024
			24	1.1686
	3320		28.5	0.9841
	4150		32	0.8765
			36.5	0.7684
			42	0.6678

Table A1. *Cont.*

Yield (MPa)	Length (mm)	Breadth (mm)	Thickness (mm)	Plate Slenderness Ratio
315	830	830	8.5	3.8202
			12	2.7060
			15.5	2.0950
	1660		18.5	1.7552
			22	1.4760
	2490		26	1.2489
			30	1.0824
	3320		34	0.9551
			38.5	0.8434
	4150		44.5	0.7297
355	830	830	9	3.8302
			12	2.8727
			17	2.0278
	1660		19	1.8143
			23	1.4988
	2490		26.5	1.3008
			30.5	1.1302
	3320		34.5	0.9992
			42	0.8208
	4150		50	0.6894

References

1. Paik, J.K.; Kim, D.K.; Kim, M.S. Ultimate strength performance of Suezmax tanker structures: Pre-CSR versus CSR designs. In *Analysis and Design of Marine Structures*; CRC Press: Boca Raton, FL, USA, 2009; pp. 205–216.
2. Paik, J.K.; Kim, B.J.; Seo, J.K. Methods for ultimate limit state assessment of ships and ship-shaped offshore structures: Part I—Unstiffened plates. *Ocean. Eng.* **2008**, *35*, 261–270. [CrossRef]
3. Paik, J.K.; Seo, J.K. Nonlinear finite element method models for ultimate strength analysis of steel stiffened-plate structures under combined biaxial compression and lateral pressure actions—Part I: Plate elements. *Thin-Walled Struct.* **2009**, *47*, 1008–1017. [CrossRef]
4. Paik, J.K. Ultimate limit state performance of oil tanker structures designed by IACS common structural rules. *Thin-Walled Struct.* **2007**, *45*, 1022–1034. [CrossRef]
5. Bäseler, W.; Bauer, G.; Dreyfus, L.; Düll, R.; Föppl, L.; Föppl, O.; v Kármán, T. Die mittragende Breite. In *Beiträge zur Technischen Mechanik und Technischen Physik: August Föppl zum Siebzigsten Geburtstag am 25. Januar 1924*; Springer: Berlin/Heidelberg, Germany, 1924; pp. 114–127.
6. Paik, J.K.; Amlashi, H.; Boon, B.; Branner, K.; Caridis, P.; Das, P.; Fujikubo, M.; Huang, C.-H.; Josefson, L.; Kaeding, P.; et al. Committee III. 1 ultimate strength. In Proceedings of the 18th International Ship and Offshore Structures Congress Schiffbautechnische Gesellschaft eV, Rostock, Germany, 9–13 September 2012; pp. 285–363.
7. Kim, D.K.; Lim, H.L.; Yu, S.Y. A technical review on ultimate strength prediction of stiffened panels in axial compression. *Ocean Eng.* **2018**, *170*, 392–406. [CrossRef]
8. Kim, D.K.; Poh, B.Y.; Lee, J.R.; Paik, J. Ultimate strength of initially deflected plate under longitudinal compression: Part I = An advanced empirical formulation. *Struct. Eng. Mech.* **2018**, *68*, 247–259.
9. Lim, H.L.; Yu, S.Y. Ultimate strength prediction of T-bar stiffened panel under longitudinal compression by data processing: A refined empirical formulation. *Ocean Eng.* **2019**, *192*, 106522.
10. Oh, S.J.; Lim, C.O.; Park, B.C.; Lee, J.C.; Shin, S.C. Deep neural networks for maximum stress prediction in piping design. *Int. J. Fuzzy Log. Intell. Syst.* **2019**, *19*, 140–146. [CrossRef]
11. Paik, J.K.; Kim, S.J.; Kim, D.H.; Kim, D.C.; Frieze, P.A.; Abbattista, M.; Vallascas, M.; Hughes, O.F. Benchmark study on use of ALPS/ULSAP method to determine plate and stiffened panel ultimate strength. In Proceedings of the 3rd Advances on Marine Structures, Hamburg, Germany, 28–30 March 2011.

12. Smith, C.S.; Davidson, P.C.; Chapman, J.C. Strength and stiffness of ships'plating under in-plane compression and tension. *R. Inst. Nav. Archit. Trans.* **1988**, *130*, 277296.
13. Park, J.S.; Fujikubo, M.; Iijima, K.; Yao, T. Prediction of the secondary buckling strength and ultimate strength of cylindrically curved plate under axial compression. In *ISOPE International Ocean and Polar Engineering Conference*; ISOPE: Mountain View, CA, USA, 2009; p. ISOPE-I.
14. Kim, J.H.; Park, D.H.; Kim, S.K.; Kim, M.S.; Lee, J.M. Experimental study and development of design formula for estimating the ultimate strength of curved plates. *Appl. Sci.* **2021**, *11*, 2379. [CrossRef]
15. Park, J.S.; Paik, J.K.; Seo, J.K. Numerical investigation and development of design formula for cylindrically curved plates on ships and offshore structures. *Thin-Walled Struct.* **2018**, *132*, 93–110. [CrossRef]
16. Kim, D.K.; Ban, I.; Poh, B.Y.; Shin, S.C. A useful guide of effective mesh-size decision in predicting the ultimate strength of flat-and curved plates in compression. *J. Ocean Eng. Sci.* **2023**, *8*, 401–417. [CrossRef]
17. Kee Paik, J.; Kyun Kim, D.; Lee, H.; Lae Shim, Y. A method for analyzing elastic large deflection behavior of perfect and imperfect plates with partially rotation-restrained edges. *J. Offshore Mech. Arct. Eng.* **2012**, *134*, 021603. [CrossRef]
18. Rodrigues, M.V. Probabilistic Characterization of the Ultimate Strength of Plates with Initial Geometrical Imperfections. Master's Thesis, Technical University of Lisbon, Lisbon, Portugal, 2011.
19. Lim, C.; Han, I.S.; Kang, J.Y.; Ban, I.J.; Lee, B.; Park, J.S.; Shin, S.C. Shear Force and Bending Moment Tuning Algorithm of Shuttle Tanker Model for Global Structural Analysis. *J. Mar. Sci. Eng.* **2023**, *11*, 1900. [CrossRef]
20. Kim, D.K.; Li, S.; Lee, J.R.; Poh, B.Y.; Benson, S.; Cho, N.K. An empirical formula to assess ultimate strength of initially deflected plate: Part 1= propose the general shape and application to longitudinal compression. *Ocean. Eng.* **2022**, *252*, 111151. [CrossRef]
21. Faulkner, D. A review of effective plating for use in the analysis of stiffened plating in bending and compression. *J. Ship Res.* **1975**, *19*, 1–17. [CrossRef]
22. Cho, S.J.; Ban, I.J.; Shin, S.C. A Novel Deep Learning Model to Predict Ultimate Strength of Ship Plates under Compression. *Appl. Sci.* **2022**, *12*, 2522. [CrossRef]
23. Hastie, T.; Tibshirani, R.; Friedman, J.H.; Friedman, J.H. *The Elements of Statistical Learning: Data Mining, Inference, and Prediction*; Springer: New York, NY, USA, 2009; Volume 2, pp. 1–758.
24. Goodfellow, I.; Bengio, Y.; Courville, A. *Deep Learning*; MIT Press: Cambridge, MA, USA, 2016.
25. Patro, S.G.O.P.A.L.; Sahu, K.K. Normalization: A preprocessing stage. *arXiv* **2015**, arXiv:1503.06462. [CrossRef]
26. Hu, Z.; Zhang, J.; Ge, Y. Handling vanishing gradient problem using artificial derivative. *IEEE Access* **2021**, *9*, 22371–22377. [CrossRef]
27. Maeno, Y.; Yamaguchi, H.; Fujii, Y.; Yao, T. Buckling/Plastic Collapse Behaviour And Strength of Bilge Circle and Its Contribution to Ultimate Longitudinal Strength of Ship's Hull Girder. In *ISOPE International Ocean and Polar Engineering Conference*; ISOPE: Mountain View, CA, USA, 2004; p. ISOPE-I.
28. Kim, D.K.; Wong, A.M.K.; Hwang, J.; Li, S.; Cho, N.K. A novel formula for predicting the ultimate compressive strength of the cylindrically curved plates. *Int. J. Nav. Archit. Ocean Eng.* **2024**, *16*, 100562. [CrossRef]